HHS Public Access

Author manuscript

Biochim Biophys Acta. Author manuscript; available in PMC 2017 February 01.

Published in final edited form as:

Biochim Biophys Acta. 2016 February ; 1858(2): 354–362. doi:10.1016/j.bbamem.2015.11.024.

INTERLEAFLET MIXING AND COUPLING IN LIQUID-DISORDERED PHOSPHOLIPID BILAYERS

Sara Capponi[1], **J. Alfredo Freites**[2], **Douglas J. Tobias**[2], and **Stephen H. White**[1,*]

[1] Department of Physiology and Biophysics and Center for Biomembrane Systems, University of California at Irvine, Irvine, California, 92697 USA

[2] Department of Chemistry and Center for Biomembrane Systems, University of California at Irvine, Irvine, California, 92697 USA

Abstract

Organized as bilayers, phospholipids are the fundamental building blocks of cellular membranes and determine many of their biological functions. Interactions between the two leaflets of the bilayer (interleaflet coupling) have been implicated in the passage of information through membranes. However, physically, the meaning of interleaflet coupling is ill defined and lacks a structural basis. Using all-atom molecular dynamics simulations of fluid phospholipid bilayers of five different lipids with differing degrees of acyl-chain asymmetry, we have examined interleaflet mixing to gain insights into coupling. Reasoning that the transbilayer distribution of terminal methyl groups is an appropriate measure of interleaflet mixing, we calculated the transbilayer distributions of the acyl chain terminal methyl groups for five lipids dioleoylphosphatidylcholine (DOPC), palmitoyloleoylphosphatidylcholine (POPC), stearoyloleoylphosphatidylcholine (SOPC), oleoylmyristoylphosphatidylcholine (OMPC), and dimyristoylphosphatidylcholine (DMPC). We observed in all cases very strong mixing across the bilayer midplane that diminished somewhat with increasing acyl-chain ordering defined by methylene order parameters. A hallmark of the interleaflet coupling idea is complementarity, which postulates that lipids with short alkyl chains in one leaflet will preferentially associate with lipids with long alkyl chains in the other leaflet. Our results suggest a much more complicated picture for thermally disordered bilayers that we call distributed complementarity, as measured by the difference in the peak positions of the *sn*-1 and *sn*-2 methyl distributions in the same leaflet.

Graphical Abstract

[*]To whom correspondence should be addressed. Dept. of Physiology and Biophysics, Medical Sciences D333, University of California at Irvine, Irvine, CA 92697-4560. stephen.white@uci.edu.

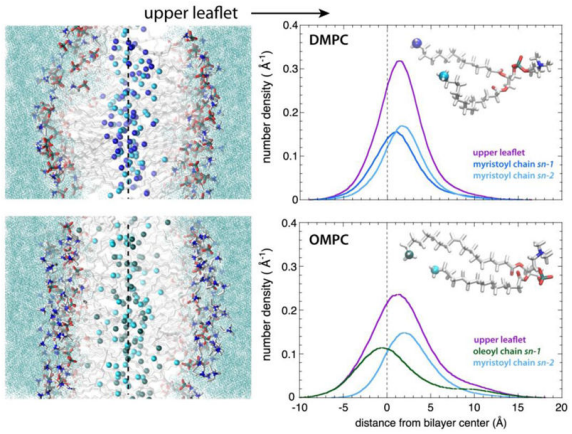

1. Introduction

Phospholipids are the dominant lipid component of cell membranes, because they are required for the formation of the bilayer matrix. Cholesterol is a significant component of the membranes of higher eukaryotes, but by itself cannot form fluid lipid bilayers. However, when cholesterol is included in liquid-disordered (l_d) phospholipid bilayers at sufficiently high concentrations, it can induce the so-called liquid-ordered (l_o) state by causing conformational ordering of the phospholipid acyl chains without loss of lipid translational mobility [1-4]. In this state, the rigid cholesterol molecule orders the acyl chains, resulting in extended conformations without entering the gel solid-ordered state (s_o). Cholesterol in the presence of two phospholipids—one with saturated alkyl chains and the other containing a double bond in one the chains—produces complex phases in which a sterol-induced l_o phase can co-exist with the l_d phase [5]. This phase behavior, the transbilayer asymmetry of lipids in native membranes [6, 7], the possibility of proteins partitioning selectively into domains in natural membranes, and the possibility that the phase behavior of each leaflet could be coupled at the membrane midplane forms the foundation of the controversial raft model [8-12].

The extent to which the two monolayer leaflets comprising a bilayer are coupled is a long-standing question originating with early studies by several laboratories [13-15]. Recent work supports the idea that the inner and outer leaflets of membrane bilayers are coupled. For example, l_o domains appear to induce ordered domain formation in inner leaflets [11, 16-23]. Interleaflet coupling apparently involves both the length and the degree of unsaturation of the acyl chains. By measuring the lateral diffusion of different lipids, Wan et al. [17] showed that interleaflet coupling is promoted in the presence of long and stretched saturated acyl chains, which might facilitate the interactions occurring in the midplane between opposite leaflets [23].

A fundamental problem is that interleaflet coupling is ill defined structurally. A simple question is whether it is possible to form a bilayer in some manner that results in completely independent behavior of the individual leaflets. This independent-leaflet idea, conceived at a time when there was little direct bilayer structural information, was the subject of the earliest

studies of interleaflet coupling [13-15]. A keystone of the interleaflet coupling idea is complementarity [24-26], which postulates that lipids with short alkyl chains in one leaflet will preferentially associate with lipids with long alkyl chains in the other leaflet. A corollary is that lipids with asymmetric chain lengths will associate across the bilayer in a way that favors the association of the short alkyl chain in one leaflet with the longer alkyl chain in the opposing leaflet. The physical chemistry of dispersions of such mixed-chain lipids has been explored extensively by Huang and Mason [27]. As might have been anticipated, the effect of complementarity was mostly apparent for lipids in the gel s_o state.

An important first step toward defining the meaning of interleaflet coupling of l_d and l_o bilayers is to define it structurally by simply determining the transbilayer distribution of the terminal methyl groups of alkyl chains of single-component lipid bilayers. That is, what fraction of methyl groups in one leaflet is found in the other? Combined x-ray and neutron diffraction studies of oriented dioleoylphosphatidylcholine (DOPC) bilayers revealed that the transbilayer distributions of most lipid components, such as phosphates and double bonds, can be described accurately as Gaussian [28]. The shape of the distribution of the terminal groups, however, was less clear. Subsequent molecular dynamics simulations showed that the transbilayer distributions of terminal methyls deviated from Gaussian functions [29-32]. The shape of the transbilayer distribution of methyl groups in oriented DOPC bilayers at low hydration (5.4 waters/lipid) was determined directly by Mihailescu et al. [33] using neutron diffraction and specific deuteration of the methyl groups. In the same study, specifically deuterated cholesterol was introduced to produce a liquid-ordered phase. In the absence of cholesterol, the methyl distribution was found to have a strong central peak with weaker 'wings' that overlapped the water distributions at the edge of the bilayer. The strong central peak was Gaussian in shape but accounted for only 80% of the methyl groups. The wings of the distribution accounted for the remaining 20% of the methyls, which led to the conclusion that the terminal methyl groups spend about 20% of their time in the bilayer interface in contact with water and polar headgroups, as hinted at by less direct methods [34-36]. In the presence of cholesterol, the wings were found to retract, consistent with the DOPC molecules being in a liquid-ordered state.

In addition to their neutron diffraction measurements, Mihailescu et al. [33] also carried out all-atom molecular dynamics (MD) simulations of their systems that produced methyl distributions that agreed with the diffraction results. Importantly, the simulations allowed the transbilayer distribution of the lipid acyl chain methyls of each leaflet to be determined. The MD simulations revealed very strong mixing of acyl chains across the bilayer mid-plane that was reduced in the presence of cholesterol. Three questions then arose. First, how is transbilayer mixing affected for lipids in excess water? Second, what is the mixing behavior when only one of the acyl chains carries a double bond? Third, how do disparities in the number of carbons in each chain affect mixing? We present here answers to those questions obtained from molecular dynamics simulations of five lipid bilayer systems in excess water, including DOPC, palmitoyloleoylphosphatidylcholine (POPC), stearoyloleoylphosphatidylcholine (SOPC), oleoylmyristoylphosphatidylcholine (OMPC), and dimyristoylphosphatidylcholine (DMPC). We were especially interested in OMPC compared to DMPC because of the large asymmetry in the acyl chain length in OMPC,

which might serve as a model for describing other class of lipids with asymmetric alkyl chains, such as sphingolipids.

2. Methods

2.1 Bilayers simulated

We performed all-atom MD simulations of five fully hydrated phospholipid bilayers (30 waters per lipid) with saturated and unsaturated chains of various lengths. For lipids with symmetrical acyl chains, we simulated 1,2-dioleoyl-*sn*-glycero-3-phosphocholine (DOPC) and 1,2-dimyristoyl-*sn*-glycero-3-phosphocholine (DMPC). For lipids with asymmetric acyl chains, we selected 18:1-14:0-PC 1-oleoyl-2-myristoyl-*sn*-glycero-3-phosphocholine (OMPC), 16:0-18:1-PC 1-palmitoyl-2-oleoyl-*sn*-glycero-3-phosphocholine (POPC), and 18:0-18:1-PC 1-stearoyl-2-oleoyl-*sn*-glycero-3-phosphocholine (SOPC) lipid bilayers. All of the bilayers consisted of 72 lipids, 36 per leaflet. For the DOPC, POPC, and DMPC lipid bilayers, we used the configurations at http://terpconnect.umd.edu/~jbklauda/research/download.html, which were generated using MD simulations with the CHARMM36 force field. We built the initial configurations of the OMPC and SOPC lipid bilayers by modifying those of DOPC and POPC, respectively.

2.1 Simulation protocols

We carried out all-atom molecular dynamics simulations in *NPT* (constant number of particles *N*, pressure *P*, and temperature *T*) ensemble with the NAMD software [37, 38], version 2.9. The CHARMM36 [39] force field was used for the lipids and the TIP3P model [40] for water. The pressure was maintained constant at 1 atm by using a flexible orthorhombic cell in conjunction with Nosé-Hoover-Langevin piston algorithm [41, 42]. The temperature was kept constant at 300 K using a Langevin dynamics scheme. The electrostatic interactions were computed by means of the smooth particle-mesh Ewald (PME) summation method [43, 44] and the short-range real-space interactions were cut off at 12 Å by using a switching function between 10 Å and 12 Å. The equation of motions were integrated with a time step of 4 fs for the long-range electrostatic forces, 2 fs for the short-range non-bonded forces, and 2 fs for the bonded forces by means of a reversible multiple time-step algorithm [45]. The SHAKE algorithm [46] was used to constrain the lengths of the bonds involving hydrogen atoms. Molecular graphics and trajectory analyses were performed with VMD 1.9.1 software package [47]. The OMPC, POPC and DMPC lipid bilayer simulations were run for 100 ns, and the DOPC and SOPC simulations for 120 ns. Coördinates were saved every 10 ps.

In order to check if the systems were equilibrated, we monitored the time evolution of the area per lipid and the cell *d*-spacing (Supplementary Figs. S1 and S2, respectively). During the last 60 ns of each simulation, these values were stable in time, indicating that the systems were equilibrated. As an additional measure to check the convergence of the simulations and to study the degree of disorder of the lipid acyl chains, we calculated the orientational order parameter S_{CH} as

$$S_{CH} = \frac{1}{2}\left\langle 3\cos^2\theta - 1 \right\rangle$$

where θ is the angle between a CH bond and the bilayer normal, and the angular brackets denote an average over time and lipid molecules. We show in Figs. S3 - S7, for each bilayer simulated, the time evolution of the S_{CH} order parameter profiles of the acyl chains of three acyl carbon atoms located at different positions within the acyl chains. Namely, we monitored the S_{CH} of C3, located close to the headgroup, of C9, located in the acyl chain middle, and of C13, near the acyl chain terminal. Together, these results confirmed that the systems were at equilibrium during the last 60 ns. We used the trajectories collected in this time window to perform the data analysis.

3. Results

3.1 General features of the lipid bilayers

The area per lipid is a fundamental structural parameter often used to validate MD simulations of lipid bilayers. This key quantity has been determined experimentally for DMPC, POPC, SOPC, and DOPC, but not for OMPC. If the lipid force field we employed is capable of accurately reproducing the area per lipid for DMPC, POPC, SOPC, and DOPC bilayers, it should be capable of accurately predicting the properties of OMPC bilayers. Shown in Fig. 1 are the areas determined from our simulations for DMPC, POPC, SOPC, and DOPC bilayers (filled symbols) along with experimental values (open symbols) from the literature [32, 48-52]. The agreement between simulations and experiments is excellent, implying that our simulation of the OMPC area is reliable. The OMPC bilayer area/lipid has a value comparable to those of the mono-unsaturated lipids POPC, DOPC, and SOPC, but is significantly larger than DMPC.

We estimated the thicknesses of the bilayers (Table 1) by computing the distance between the peaks of the transbilayer distributions of the carbonyls and the phosphate groups, which are displayed in Fig. 2A. Despite the acyl chain asymmetries of OMPC, the carbonyl-to-carbonyl and the phosphate-to-phosphate distances of OMPC are similar to those of DMPC, but 2 - 4 Å smaller than those of the mono- or di-unsaturated lipid bilayers. The presence of the long, unsaturated oleoyl chain in OMPC in place of the short, saturated myristoyl chain of DMPC hardly affects the bilayer thickness, but increases the area per lipid substantially (Fig. 1). This indicates that the OMPC acyl chains are more disordered than those in DMPC, consistent with the broader methyl distribution of OMPC.

Because acyl chain order-parameter profiles are important indicators of both thickness and area/lipid, we calculated the orientational order parameters S_{CH} for each lipid (Fig. 2B). Our results for DMPC, POPC and DOPC bilayers are in good agreement with those summarized by Poger et al. [53]. The general features of the order parameter profiles are quite similar for SOPC and POPC, but dramatically different for OMPC. In OMPC, the S_{CH} profile of the *sn*-1 chain reaches a low value of about 0.05 near the center of the chain, which is similar to the profiles for SOPC and DOPC, but has significantly lower order close the headgroup.

3.2 The sn-1 and sn-2 terminal methyl groups of all five lipids explore the water-membrane interface

The transbilayer distributions of the methyl ends of the acyl chains are good measures of mixing between the opposing monolayers and, hence, interleaflet coupling. The transbilayer distributions of methyl groups of the five bilayers are shown in Fig. 3 as solid black lines. In all of the systems, the distributions show a strong central peak with lateral shoulders, the extension and intensity of which vary with the chemical structure of the lipids. The shoulders, which as previously noted represent a departure from Gaussian distributions [29-31], are pronounced in all of oleyl-containing lipid bilayers and almost absent in the DMPC bilayer. In all of the systems, the acyl chains are able to bend back such that the terminal methyl groups make excursions toward the bilayer-water interface. To estimate the extent of backward bending of the different lipids, and to quantify the deviation from a normal distribution, we fitted the central regions of transbilayer methyl distributions with Gaussian functions, represented with dashed black curves in Fig. 3. By subtracting the area under the central Gaussians functions from the methyl distributions, we estimated for each system the fraction of the terminal methyl groups exploring the lipid-water interface with respect to the total number of the terminal methyl groups (first column of Table 2).

In the fully hydrated DOPC bilayer, 8.8% of the terminal methyl groups (Table 2) are able to explore the interface region as marked by the mean positions of the carbonyl group distributions (arrows, Fig. 3), which are a good measure of the water/hydrocarbon interface [28]. This amounts to about 6.3 terminal methyl groups for the lipid bilayer formed by 72 lipid molecules. The fraction of terminal methyl groups in the interface decreases when the acyl chain order increases. For example, there are on average 2.3 terminal methyl groups exploring the interface in our DMPC simulation. The absence of double bonds makes the saturated chains in DMPC more ordered with respect to the other systems investigated (Fig. 2). OMPC, POPC, and SOPC, each with one saturated and one unsaturated chain, have values (Table 2) of the interfacial fraction of methyl groups (5.0-7.0%) that are intermediate between those of DMPC (3.2%) and DOPC (8.8%).

Because the saturated acyl chains are more ordered and less flexible than the unsaturated chains, they might contribute less to the presence of terminal methyl groups in the interface. To test this hypothesis, we calculated for each bilayer the transbilayer distributions of the *sn-1* and *sn-2* acyl chains separately, and plotted them along with the total methyl group distributions in Fig. 3. It is evident that the presence of the terminal methyl groups in the interface depends on both the structures of the acyl chains and of the lipid molecules. Following the procedure used for the total methyl group distributions, we fitted the *sn-1* and *sn-2* acyl chain distributions with Gaussian functions and determined by subtraction the contributions of *sn-1* and *sn-2* terminal methyl groups to the populations of terminal methyl groups located near the membrane-water interface (Table 2). In the DOPC bilayer, the *sn-1* and *sn-2* chains contribute almost equally to the presence of the terminal methyl groups near the interface. This finding is in agreement with the S_{CH} profiles (Fig. S2) in which the DOPC unsaturated oleoyl chains exhibit similar order-parameter profiles. The unsaturated oleoyl chain gains flexibility when it is associated with a shorter saturated acyl chain, as in the cases of SOPC, POPC, and OMPC. The percentage of the oleoyl methyl groups in the

interface with respect to the total number of methyl groups increases from 50% in DOPC to ~65% in SOPC and POPC, and 74% in OMPC. The degree of disorder exhibited by the *sn-1* oleoyl chain in OMPC is comparable to that exhibited by the *sn-1* oleoyl chain in DOPC (Fig. 2B). On the other hand, the short *sn-2* saturated myristoyl chain in OMPC is more disordered than the corresponding acyl chain in DMPC (Fig. 2B). The ability of a given acyl chain to bend backward toward the membrane-water interface is reduced when the chain is associated with a longer unsaturated chain, as in DOPC, rather than with a saturated chain of the same length, as in DMPC.

3.3 Interleaflet mixing and coupling

The key issue for understanding interleaflet coupling is the extent to which terminal groups mix across the bilayer midplane. To examine this question, we calculated the distributions of the terminal methyl groups belonging to each bilayer leaflet. These distributions are plotted in Fig. 4 ("upper" leaflet in *violet*, "lower" leaflet in *magenta*) along with the total terminal methyl distributions and the corresponding Gaussian fitting functions (Fig. 4, solid and dashed black lines, respectively). In all of the systems, both the upper and lower leaflet distributions are asymmetric. They exhibit a peak close to the bilayer center with a shoulder that extends into the corresponding membrane-water interface (marked by small arrows; see also Fig. 2A). The shoulders are more pronounced in unsaturated or mixed unsaturated/saturated lipid bilayers. The broadest shoulders are found in the DOPC bilayer, whose acyl chains have the highest conformational disorder due to the presence of two double bonds (Fig. 2B). The smallest shoulders are observed in the leaflet distributions for the DMPC bilayer, which has the most ordered chains (Fig. 2B), causing the methyl groups to be more localized. The degree of mixing between opposite leaflets is overall very high, as indicated by the gray overlap zones. The upper and lower leaflet distributions overlap substantially in all the systems, ranging from 71% for DOPC to 57% for DMPC (Table 3). The overlap of the leaflet distributions decreases in the order DOPC > SOPC > POPC > OMPC > DMPC. Interestingly, for the lpids considered here, the overlap seems to correlate roughly with the number of lipid acyl-chain carbons, perhaps simply because longer chains have more conformational degrees of freedom. In any case, overall, these findings are consistent with our earlier results for DOPC bilayers at low hydration in the absence and presence of cholesterol [33]; adding cholesterol increased acyl chain order and decreased the mixing between opposite lipid layers.

To analyze more quantitatively the degree of the interleaflet mixing based on the area shared by the upper and lower leaflet distributions, we calculated the number of terminal methyl groups that one leaflet shares with the opposite one (Table 3). These "interacting areas", colored grey in Fig. 4, correspond to the zone in the middle of the bilayer where it is possible to find methyl groups belonging to both the upper and lower leaflets and therefore where opposing acyl chains interact. Each DOPC lipid molecule shares 1.42 methyl groups out of 2 with the opposite leaflet, which corresponds to about the 70% of the total methyl groups of a leaflet. The interleaflet mixing decreases remarkably in the DMPC bilayer, in which the percentage of the terminal methyl groups shared by each leaflet reaches only the 57% (each lipid molecule shares only 1.14 out of 2 terminal methyl groups with the opposite leaflet). Another measure of interleaflet mixing is the distance between the methyl group

peaks of opposing leaflets. This distance corresponds to the distance between the main peaks of the transbilayer distribution of opposite leaflet: As the interleaflet mixing decreases, the distance between opposing terminal methyl group peaks increase: 0.6 Å in DOPC, 2.2 Å in SOPC and POPC, and 2.8 Å in OMPC and DMPC bilayers, respectively.

Is there is any evidence of complementarity in these highly disordered bilayers, all of which have very significant interleaflet mixing? To examine that question, we calculated the transbilayer distributions of the *sn-1* and *sn-2* methyl groups of the "upper" leaflets (Fig. 5, right-hand panel); the corresponding distributions for the "lower" leaflets are essentially identical. The left-hand panels of Fig. 5 show representative snapshots of the bilayers color-coded as in Fig. 3. The conformation of the headgroup of phosphorylcholine lipids is such that the glycerol backbone is aligned roughly normal to the bilayer [54-56]. Because natural asymmetric phosphocholine lipids generally have the shorter acyl chain in the *sn*-1 position, e.g. POPC, the glycerol orientation effectively extends the *sn-1* chain two methylenes deeper into bilayer so that the methyl is at same level as the methyl of the longer acyl chain in the *sn-2* position. This is apparent from the upper leaflet profiles of POPC and DMPC. For POPC, the upper leaflet methyl distributions are have nearly overlapping maxima whereas for DMPC *sn*-2 methyl peak is closer to interface than the *sn*-1 peak, consistent with the effect of the glycerol orientation and acyl chain asymmetry. Similarly to DMPC, the *sn*-2 methyl peak of DOPC is closer to the interface than the *sn*-1 methyl. The situation for OMPC and SOPC is quite different; the peak separations of the *sn*-1 and *sn*-2 methyls are much larger than for DMPC, POPC, and DMPC. These results reveal what might be called thermally disordered or distributed complementarity in the bilayer structure. Notice that for all of the profiles shown in Fig. 3, the methyls are symmetrically distributed across the bilayer. The complementarity is only apparent when the distributions of the methyls of individual leaflets are examined.

4. Discussion

Our systematic analyses of the distributions of acyl chain terminal methyl groups within five fully hydrated phospholipid bilayers, with variable chain lengths and saturation, provide a clearer understanding of the interleaflet mixing and coupling. In all of the systems investigated, both saturated and unsaturated acyl chains display a high degree of conformational flexibility, enabling the terminal methyl groups to explore the water-membrane interface to different extents that depend upon relative chain lengths, acyl chain asymmetry, and the presence of double-bonds (Fig. 3 and Table 2). In general, the ‘bending back’ of methyls to the membrane interface is greater for acyl chains carrying a double bond (compare *sn*-1 and *sn*-2 in Table 2). Our results show that under all circumstances there is a large amount of interleaflet mixing, ranging from 57% for DMPC to 71% for DOPC (Table 3). The degree of mixing across the bilayer midplane depends upon the number of lipid carbon atoms, the presence of double bonds, and acyl chain asymmetry (Fig. 4 and Table 3). The early idea that the monolayers of bilayers might act independently [13] is clearly not correct; the two monolayers of l_d bilayers appear to be structurally coupled through interleaflet mixing.

A major line of thought in recent literature regarding interleaflet coupling is lipid complementarity, which postulates that lipids with short alkyl chains in one leaflet will preferentially associate with lipids with long alkyl chains in the other leaflet [24-26]. Our results suggest a much more complicated picture that we call thermally disordered or distributed complementarity. This is measured by the difference in the peak positions of the *sn*-1 and *sn*-2 methyl distributions in the same leaflet (Fig. 5). Our results are consistent with the fact that the glycerol backbone is aligned roughly normal to the bilayer [54-56]. This is apparent from the upper leaflet profiles of POPC and DMPC. For POPC, the upper leaflet methyl distributions are have nearly overlapping maxima whereas for DMPC *sn*-2 methyl peak is closer to interface than the *sn*-1 peak, consistent with the effect of the glycerol orientation and acyl chain asymmetry. Similarly to DMPC, the *sn*-2 methyl peak of DOPC is closer to the interface than the *sn*-1 methyl. The situation for OMPC and SOPC is quite different; the peak separations of the *sn*-1 and *sn*-2 methyls are much larger than for DMPC, POPC, and DMPC. We do not envision direct complementarity between directly opposed lipids in the two leaflets, but rather distributed complementarity in which the only rule is that partial specific volumes of methylenes and methyls are fixed to assure uniform acyl chain packing.

We observed in an earlier study [33] of DOPC bilayers at low hydration that the introduction of cholesterol to produce l_o bilayers caused the methyl groups to retract from the interface. Nevertheless, considerable interleaflet mixing of the DOPC acyl chains was observed. The effect of cholesterol on the transbilayer methyl distributions reported here remains to be established.

Supplementary Material

Refer to Web version on PubMed Central for supplementary material.

Acknowledgements

We thank Dr. Salvatore Chiantia and Prof. Erwin London for their encouragement to pursue these simulations. We thank Swati Rawat for her help in the early stages of the simulations. This research was supported by grants from the National Institutes of Health (RO1 GM74637 to S. H. W.) and (PO1 GM86685 to D. J. T. and S. H. W.). The simulations were performed on the High Performance Computing (HPC) cluster at the University of California, Irvine. We thank Joseph Farran for excellent technical support.

References

1. Lecuyer H, Dervichian DG. Structure of aqueous mixtures of lecithin and cholesterol. J. Mol. Biol. 1969; 45:39–57. [PubMed: 5343454]
2. Levine YK, Wilkins MHF. Structure of oriented lipid bilayers. Nature New Biol. 1971; 230(11):69–76. [PubMed: 5279040]
3. Rothman JE, Engelman DM. Molecular mechanism for the interaction of phospholipid with cholesterol. Nature New Biol. 1972; 237(71):42–44. [PubMed: 4503742]
4. Sankaram MB, Thompson TE. Cholesterol-induced fluid-phase immiscibility in membranes. Proc. Natl. Acad. Sci. U.S.A. 1991; 88:8686–8690. [PubMed: 1656453]
5. Feigenson GW. Phase behavior of lipid mixtures. Nat. Chem. Biol. 2006; 2(11):560–563. [PubMed: 17051225]
6. Bretscher MS. Asymmetrical lipid bilayer structure for biological membranes. Nature New Biology. 1972; 236:11–20. [PubMed: 4502419]

7. Rothman JE, Lenard J. Membrane asymmetry. The nature of membrane asymmetry provides clues to the puzzle of how membranes are assembled. Science. 1977; 195:743–753. [PubMed: 402030]
8. Simons K, Toomre D. Lipid rafts and signal transduction. Nat. Rev. Mol. Cell Biol. 2000; 1:31–39. [PubMed: 11413487]
9. Van Meer G, Voelker DR, Feigenson GW. Membrane lipids: where they are and how they bahave. Nature Rev. Mol. Cell Biol. 2008; 9:112–124. [PubMed: 18216768]
10. Lingwood D, et al. Lipid rafts as functional heterogeneity in cell membranes. Biochem. Soc. Trans. 2009; 37:955–960. [PubMed: 19754431]
11. Simons K, Gerl MJ. Revitalizing membrane rafts: new tools and insights. Nat. Rev. Mol. Cell. Biol. 2010; 11:688. [PubMed: 20861879]
12. Kraft ML. Plasma membrane organization and function: moving past lipid rafts. Molecular Biology of Cell. 2013; 24:2765–2768.
13. Sillerud LO, Barnett RE. Lack of transbilayer coupling in phase transitions of phosphatidylcholine vesicles. Biochemistry. 1982; 212:1756–1760. [PubMed: 6896282]
14. Schmidt CF, et al. Monolayer coupling in sphingomyelin bilayer systems. Nature. 1978; 271(5647):775–777. [PubMed: 625351]
15. Duzgunes N, et al. Monolayer coupling in phosphatidylserine bilayers: Distinct phase transitions induced by magnesium interacting with one or both monolayers. Biochim. Biophys. Acta. 1988; 944:391–398. [PubMed: 3179295]
16. Brown DA, London E. Structure and function of sphingolipid- and cholesterol-rich membrane rafts. J. Biol. Chem. 2000; 275(23):17221–17224. [PubMed: 10770957]
17. Wan C, Kiessling V, Tamm LK. Coupling of cholesterol-rich lipid phases in asymmetric bilayers. Biochemistry. 2008; 47:2190–2198. [PubMed: 18215072]
18. Collins MD, Keller S. Tuning lipid mixtures to induce or suppress domain formation across leaflets of unsupported asymmetric bilayers. Proc. Natl. Acad. Sci. U.S.A. 2008; 105:124–128. [PubMed: 18172219]
19. Hamada T, et al. Construction of asymmetric cell-sized lipid vesicles from lipid-coated water-in-oil microdroplets. J. Phys. Chem. B. 2008; 112:14678–14681. [PubMed: 18983183]
20. Kiessling V, Wan C, Tamm LK. Domain coupling in asymmetric lipid bilayers. Biochim. Biophys. Acta. 2009; 1788:64–71. [PubMed: 18848518]
21. May S. Trans-monolayer coupling of fluid domains in lipid bilayers. Soft Matter. 2009; 5:3148–3156.
22. Putzel GG, et al. Interleaflet coupling and domain registry in phase-separated lipid bilayers. Biophys. J. 2011; 100:996–1004. [PubMed: 21320444]
23. Chiantia S, London E. Acyl chain length and saturation modulate interleaflet coupling in asymmetric bilayers: effects on dynamics and structural order. Biophys. J. 2012; 103:2311–2319. [PubMed: 23283230]
24. Zhang J, et al. Transbilayer complementarity of phospholipids. A look beyond the fluid mosaic model. J. Am. Chem. Soc. 2004; 126:10856–10857. [PubMed: 15339166]
25. Zhang J, Jing B, Regen SL. Transbilayer complementarity of phospholipids. Proof of principle. Langmuir. 2005; 21(20):8983–8996. [PubMed: 16171319]
26. Zhang J, et al. Transbilayer complementarity of phospholipids in cholesterol-rich membranes. Biochemistry. 2005; 44:3598–3603. [PubMed: 15736969]
27. Huang C-H, Mason JT. Structure and properties of mixed-chain phospholipid assemblies. Biochim. Biophys. Acta. 1986; 864:423–471. [PubMed: 3539195]
28. Wiener MC, White SH. Structure of a fluid dioleoylphosphatidylcholine bilayer determined by joint refinement of x-ray and neutron diffraction data. III. Complete structure. Biophys. J. 1992; 61:434–447. [PubMed: 1547331]
29. Feller SE, et al. Molecular dynamics simulation of unsaturated lipid bilayers at low hydration: Parameterization and comparison with diffraction studies. Biophys. J. 1997; 73(5):2269–2279. [PubMed: 9370424]
30. Benz RW, et al. Experimental validation of molecular dynamics simulations of lipid bilayers: A new approach. Biophys. J. 2005; 88:805–817. [PubMed: 15533925]

31. Klauda JB, et al. Simulation-based methods for interpreting x-ray data from lipid bilayers. Biophys. J. 2006; 90:2796–2807. [PubMed: 16443652]
32. Kucerka N, et al. Lipid bilayer structure determined by the simultaneous analysis of neutron and x-ray scattering data. Biophys. J. 2008; 95:2356–2367. [PubMed: 18502796]
33. Mihailescu M, et al. Acyl-chain methyl distributions of liquid-ordered and -disordered membranes. Biophys. J. 2011; 100:1455–1462. [PubMed: 21402027]
34. Xu Z-C, Cafiso DS. Phospholipid packing and conformation in small vesicles revealed by two-dimensional ^{1}H nuclear magnetic resonance cross-relaxation spectroscopy. Biophys. J. 1986; 49:779–783. [PubMed: 3754469]
35. Forbes J, Husted C, Oldfield E. High-field, high-resolution proton "magic angle" sample-spinning nuclear magnetic resonance spectroscopic studies of gel and liquid crystalline lipid bilayers and effects of cholesterol. Journal of American Chemical Society. 1988; 110:1059–1065.
36. Huster D, Gawrisch K. NOESY NMR crosspeaks between lipid headgroups and hydrocarbon chains: Spin diffusion or molecular disorder? J. Am. Chem. Soc. 1999; 121:1992–1993.
37. Kalé L, et al. NAMD2: Greater scalability for parallel molecular dynamics. J. Comput. Phys. 1999; 151:283–312.
38. Phillips JC, et al. Scalable molecular dynamics with NAMD. J. Comput. Chem. 2005; 26:1781–1802. [PubMed: 16222654]
39. Klauda JB, et al. Update of the CHARMM all-atom additive force field for lipids: validation on six lipid types. J. Phys. Chem. B. 2010; 114:7830–7843. [PubMed: 20496934]
40. Jorgensen WL, et al. Comparison of simple potential functions for simulating liquid water. J. Chem. Phys. 1983; 79(2):926–935.
41. Martyna GJ, Tobias DJ, Klein ML. Constant-pressure molecular-dynamics algorithms. J. Chem. Phys. 1994; 101:4177–4189.
42. Feller SE, et al. Constant pressure molecular dynamics simulation: The Langevin piston method. J. Chem. Phys. 1995; 103(11):4613–4621.
43. Darden T, York D, Pedersen L. Particle mesh Ewald: An N•log(N) method for Ewald sums in large systems. J. Chem. Phys. 1993; 98:10089–10092.
44. Essmann U, et al. A smooth particle mesh Ewald method. J. Chem. Phys. 1995; 103:8577–8593.
45. Grubmüller H, et al. Generalized Verlet algorithm for efficient molecular dynamics simulations with long-range interactions. Mol. Simul. 1991; 6:121–142.
46. Ryckaert J-P, Ciccotti G, Berendsen HJC. Numerical integration of the Cartesian equations of motion of a system with constraints: Molecular dynamics of n-alkanes. J. Comput. Phys. 1977; 23:327–341.
47. Humphrey W, Dalke W, Schulten K. VMD: Visual molecular dynamics. J. Mol. Graph. 1996; 14(1):33–38. [PubMed: 8744570]
48. Luzzati V, Husson F. The structure of the liquid-crystalline phases of lipid-water systems. J. Cell Biol. 1962; 12:207–219. [PubMed: 14467542]
49. Koenig BW, Strey HH, Gawrisch K. Membrane lateral compressibility determined by NMR and x-ray diffraction: Effect of acyl chain polyunsaturation. Biophys. J. 1997; 73(4):1954–1966. [PubMed: 9336191]
50. Nagle JF, Tristram-Nagle S. Structure of lipid bilayers. Biochim. Biophys. Acta. 2000; 1460:159–195. [PubMed: 11063882]
51. Kučerka N, Tristram-Nagle S, Nagle JF. Structure of fully hydrated fluid phase lipid bilayers with monounsaturated chains. J. Membr. Biol. 2005; 208:193–202. [PubMed: 16604469]
52. Kučerka N, Nieh M-P, Katsaras J. Fluid phase lipid areas and bilayer thicknesses of commonly used phosphatidylcholines as a function of temperature. Biochim. Biophys. Acta. 2011; 1808:2761–2771. [PubMed: 21819968]
53. Poger D, Mark AE. On the validation of molecular dynamics simulations of saturated and cis-monounsaturated phosphatidylcholine lipid bilayers: A comparison with experiment. J. Chem. Theor. Comput. 2010; 6:325–336.

54. Hitchcock PB, et al. Structural chemistry of 1,2 dilauroyl-DL-Phosphatidylethanolamine: Molecular conformation and intermolecular packing of phospholipids. Proc. Natl. Acad. Sci. U.S.A. 1974; 71(8):3036–3040. [PubMed: 4528741]

55. Hauser H, et al. Preferred conformation and molecular packing of phosphatidylethanolamine and phosphatidylcholine. Biochim. Biophys. Acta. 1981; 650:21–51. [PubMed: 7020761]

56. Hong M, Schmidt-Rohr K, Zimmermann H. Conformational constraints on the headgroup and sn-2 chain of bilayer DMPC from NMR dipolar couplings. Biochemistry. 1996; 35:8335–8341. [PubMed: 8679591]

Highlights

- Molecular dynamics simulations were carried out on fluid bilayers in excess water using five different diacylglycerophospholipids with symmetric and asymmetric acyl chains to examine interleaflet mixing.
- Interleaflet mixing, defined by the extent of overlap of the methyl groups in opposing bilayer leaflets, was high in all cases and ranged from 57% to 71%.
- We introduce the idea of distributed complementarity for thermally disordered bilayers formed from lipids with asymmetric acyl chains.
- Distributed complementarity is quantitated by the difference in the peak positions of the *sn*-1 and *sn*-2 methyl distributions in the same leaflet.

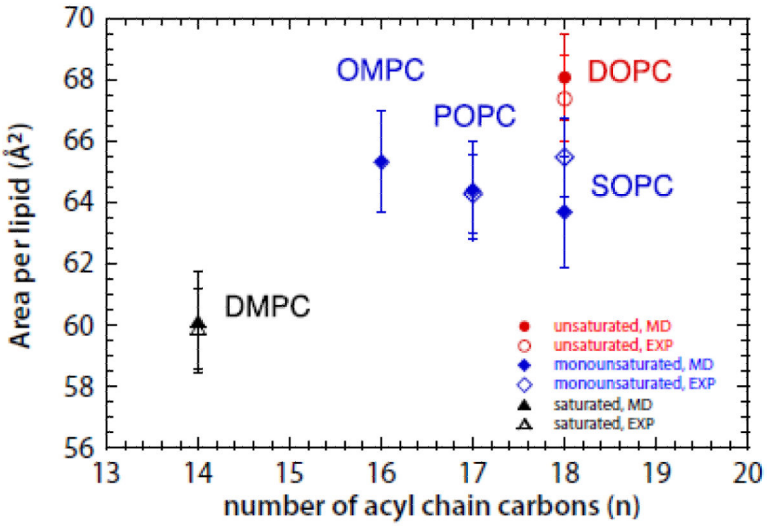

Figure 1.

Area per lipid plotted as a function of the average number *n* of the acyl carbons and displayed with symbols colored according to the degree of unsaturation of the lipid. The fully saturated lipid (DMPC) is represented with *black* triangle, the lipids with one mono-unsaturated chain and one saturated chain (OMPC, POPC and SOPC) with *blue* diamonds, and the lipid with two mono-unsaturated chains (DOPC) with *red* circles. Simulation data are represented with filled symbols, experimental data with empty symbols. The error bars are the standard deviation from the mean values.

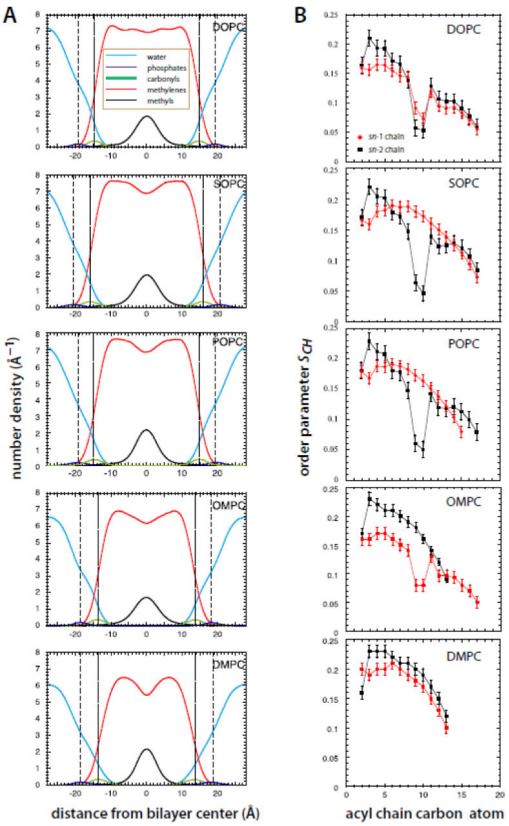

Figure 2.

Structures and order parameter profiles of the five lipid systems studied. **A**. Transbilayer distributions of the lipid component groups (see legend) for the lipid bilayers simulated in this study. Dashed lines indicate the mean position of the phosphate groups and the dotted lines the mean position of the carbonyl groups. Note that the positions of the carbonyl groups approximate the locations of the water/hydrocarbon interface, marked with arrows in Figs. 3 and 4. Areas under of purple, green, and black curves equal the number of component groups: 1 PO_4, 2 COO, 4 CH_3. Areas under red curves equal the number of non-methyl acyl chain carbons. Areas under blue curves equal the number (30) of waters/lipid. The positions of the atoms were computed at 10 ps intervals and averaged. For the phosphates and carbonyls, the distributions were fit with Gaussian functions. **B**. Order parameter profiles for the *sn*-1 (red) and *sn*-2 (black) acyl chains for DOPC, SOPC, POPC, OMPC, and DMPC lipid bilayers. See Methods. Order parameters were calculated at 10 ps intervals for the last 60 ns of the simulations and averaged. The error bars are the computed standard errors of the mean.

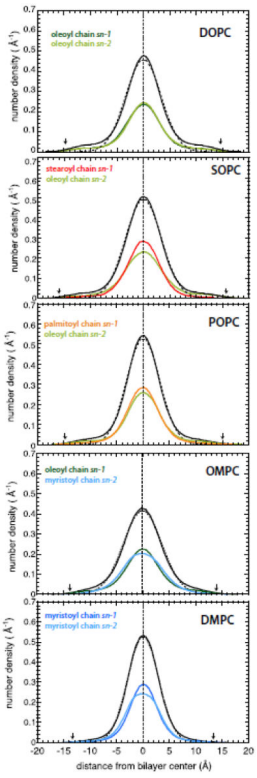

Figure 3.

Transbilayer distributions of the methyl groups of the various lipids. The transbilayer distributions of all terminal methyl groups in DOPC, SOPC, POPC, OMPC and DMPC bilayers are plotted with *solid black* lines and the corresponding Gaussian fitting functions with *dashed black* lines. The transbilayer distributions of the oleoyl acyl chain are represented in *green*, the stearoyl chain in *red*, the palmitoyl in *orange*, and the myristoyl in *blue*. The *sn-1* and the *sn-2* acyl chains are displayed in the *darker* and *brighter* color tones, respectively.

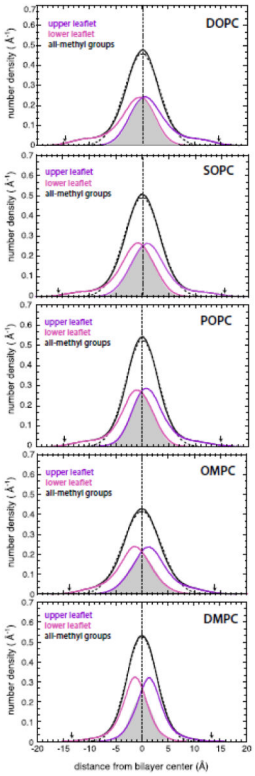

Figure 4.

Transbilayer mixing of methyl groups in the center of the bilayers. The transbilayer distributions of the terminal methyl groups belonging to the lower and upper leaflet of DOPC, SOPC, POPC, OMPC and DMPC lipid bilayers are plotted with *magenta* and *violet* lines. The transbilayer distributions of all terminal methyl groups (*solid black* lines) and the corresponding Gaussian fitting functions (*dashed black* lines) are also displayed. The degree of mixing between opposite leaflets is indicated by the gray overlap zones.

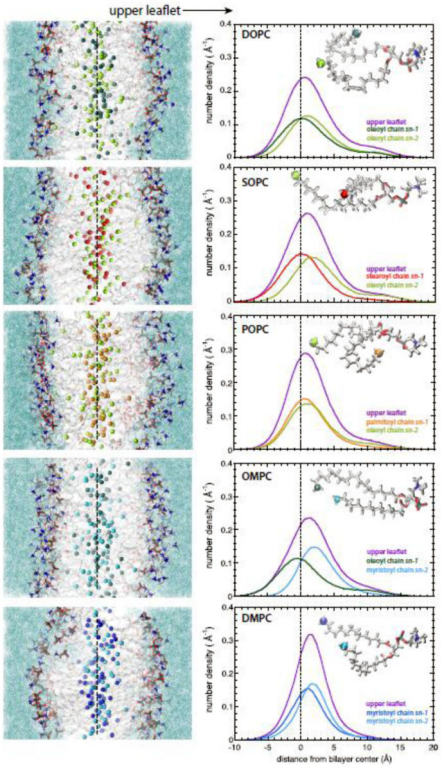

Figure 5.

Interleaflet mixing and coupling as revealed by the transbilayer methyl distributions of single leaflets. Left panel: Representative snapshots of all-atom molecular dynamics simulations of DOPC, SOPC, POPC, OMPC and DMPC lipid bilayers. The dotted line roughly indicates the middle of the bilayer. The 'upper leaflet' referred to in the right-hand panel is labeled. The terminal methyl groups are shown as spheres colored following to the scheme previously defined. The acyl chains are in *grey* stick representation; phosphocholine groups are in stick format and colored according to the element (oxygen, *red*; nitrogen, *blue*; phosphorous, *gold*; hydrogen, *white*). Water is shown as *aquamarine* solvent. Right panel: The transbilayer distributions of the terminal methyl groups belonging to the upper leaflet of DOPC, SOPC, POPC, OMPC and DMPC lipid bilayers are displayed along with those of the terminal methyl groups belonging to the *sn-1* and *sn-2* acyl chains. The distributions are colored according to the code previously defined (upper leaflet, *violet*; oleoyl chain, *green*; stearoyl chain, *red*; palmitoyl chain, *orange*; myristoyl chain, *blue*; *sn-1* and s*n-2* in *dark* and *bright* colors).

TABLE 1

Thicknesses of the phospholipid bilayers investigated. For each lipid bilayer, we calculated the number density of the carbonyls and the phosphate groups by computing the positions of the corresponding groups over all the last 60 ns of each simulation. The positions of the atoms were computed at 10 ps intervals and averaged. For the phosphates and carbonyls, the distributions were fit with Gaussian functions to estimate the mean positions and standard deviations of the mean. Distances shown in the table correspond to the distance between the two peaks located in the opposite leaflets obtained by doubling the mean position of each distribution and using the widths of the distributions to compute the standard deviations.

Lipid Bilayer	Carbonyl-Carbonyl (Å)	Phosphate-Phosphate (Å)
DOPC	29.4 ± 2.8	38.6 ± 2.8
SOPC	31.6 ± 2.9	40.9 ± 3.2
POPC	29.6 ± 3.1	38.9 ± 3.1
OMPC	27.6 ± 3.1	36.8 ± 3.0
DMPC	26.8 ± 3.4	36.2 ± 3.4

TABLE 2

Exploration of the hydrocarbon/water interface by the terminal methyl groups. The percentages of the terminal methyl groups exploring the polar region, calculated by subtracting from the total area under the distribution the area under the Gaussian function fitted to the central peak, are listed in the first column. The percentages (numbers) of the *sn-1* and *sn-2* acyl chain terminal methyl groups able to explore the interface. In each column, the average numbers of methyl groups in the simulation cell of 72 lipids exploring the interface is indicated in parentheses.

Bilayer	terminal methyl groups in the interface	*sn-1*	*sn-2*
DOPC	8.8 % (~ 6.3)	48% (~ 3.1)	52% (~ 3.2)
SOPC	6.6 % (~ 4.7)	35% (~ 1.6)	65% (~ 3.1)
POPC	7.0 % (~ 5.0)	37% (~ 1.8)	63% (~ 3.2)
OMPC	5.0 % (~ 3.6)	83% (~ 3.0)	17% (~ 0.6)
DMPC	3.2 % (~2.3)	62% (~1.4)	38% (~0.9)

Table 3

Sharing of terminal methyl groups between bilayer leaflets. We report in the first column the total number of carbon atoms of the acyl chains of each lipid bilayer we investigated; in the second column the number of the terminal methyl groups of a lipid molecule shared by each leaflet calculated by subtracting from the total area of the upper (lower) leaflet terminal methyl distributions the area shared with the lower (upper) leaflet terminal methyl distributions; in the third column the percentage of the terminal methyl groups of each leaflet shared with the opposite leaflet are shown.

Bilayer	total numbers of carbons in acyl chains	number of methyl C atoms shared by each leaflet per lipid molecule	% methyl C atoms shared with the opposite leaflet
DOPC	36	1.42	71.0
SOPC	36	1.39	69.5
POPC	34	1.30	65.0
OMPC	32	1.27	63.5
DMPC	28	1.14	57.0